epl A Letters Journal Exploring the Frontiers of Physics

November 2007

EPL, **80** (2007) 34002
doi: 10.1209/0295-5075/80/34002

www.epljournal.org

Non–Oberbeck-Boussinesq effects in two-dimensional Rayleigh-Bénard convection in glycerol

K. Sugiyama[1], E. Calzavarini[1], S. Grossmann[2] and D. Lohse[1]

[1] *Physics of Fluids group, Department of Applied Physics, J. M. Burgers Centre for Fluid Dynamics, and Impact-, MESA-, and BMTI-Institutes, University of Twente - P. O. Box 217, 7500 AE Enschede, The Netherlands*
[2] *Fachbereich Physik der Philipps-Universitaet - Renthof 6, D-35032 Marburg, Germany*

received 1 July 2007; accepted in final form 3 September 2007
published online 28 September 2007

PACS 47.27.te – Turbulent convective heat transfer
PACS 47.20.Bp – Buoyancy-driven instabilities (*e.g.*, Rayleigh-Bénard)
PACS 47.27.ek – Direct numerical simulations

Abstract – We numerically analyze Non–Oberbeck-Boussinesq (NOB) effects in two-dimensional Rayleigh-Bénard flow in glycerol, which shows a dramatic change in the viscosity with temperature. The results are presented both as functions of the Rayleigh number Ra up to 10^8 (for fixed temperature difference Δ between the top and bottom plates) and as functions of Δ ("non-Oberbeck-Boussinesqness" or "NOBness") up to 50 K (for fixed Ra). For this large NOBness the center temperature T_c is more than 5 K larger than the arithmetic mean temperature T_m between top and bottom plate and only weakly depends on Ra. To physically account for the NOB deviations of the Nusselt numbers from its Oberbeck-Boussinesq values, we apply the decomposition of Nu_{NOB}/Nu_{OB} into the product of two effects, namely first the change in the sum of the top and bottom thermal BL thicknesses, and second the shift of the center temperature T_c as compared to T_m. While for water the origin of the Nu deviation is totally dominated by the second effect (cf. Ahlers G. *et al.*, *J. Fluid Mech.*, **569** (2006) 409) for glycerol the *first* effect is dominating, in spite of the large increase of T_c as compared to T_m.

Introduction. – In most theoretical and numerical studies on Rayleigh-Bénard (RB) convection, the Oberbeck-Boussinesq (OB) approximation [1,2] is employed, *i.e.*, the fluid material properties are assumed to be independent of temperature T except for the density in the buoyancy term which is taken to be linear in T. The problem has two control parameters, namely the Rayleigh number $Ra = \beta g L^3 \Delta/(\kappa\nu)$ (here β is the thermal expansion coefficient, g the gravitational acceleration, L the height, Δ the temperature difference between bottom and top plates, κ the thermal diffusivity, and ν the kinematic viscosity), and the Prandtl number $Pr = \nu/\kappa$. For the OB case the mean temperature profile shows top-bottom symmetry. However, in real fluids, if Δ is large, this symmetry no longer holds due to the temperature dependences of the material properties. Thus, for given fluid, Δ appears as an additional control parameter, which characterizes the deviations from OB conditions, leading to so-called Non-Oberbeck-Boussinesq (NOB) effects. The NOB signatures can be quantified by i) a shift $T_c - T_m$ of the bulk (or center) temperature T_c from the arithmetic mean temperature T_m between the bottom and top plates and ii) by the ratio of the Nusselt numbers Nu_{NOB}/Nu_{OB} in the NOB and OB cases, which deviates from one. Both quantities have been measured in the large Ra regime for helium [3], glycerol [4], ethane [5], and water [6] as functions of the NOB-ness Δ.

As shown in Ahlers *et al.* [6] the Nusselt number ratio Nu_{NOB}/Nu_{OB} can be connected to T_c by the identity

$$\frac{Nu_{NOB}}{Nu_{OB}} = \frac{2\lambda_{OB}^{sl}}{\lambda_t^{sl}+\lambda_b^{sl}} \cdot \frac{\kappa_t\Delta_t + \kappa_b\Delta_b}{\kappa_m\Delta} =: F_\lambda \cdot F_\Delta. \quad (1)$$

Here the labels on material properties indicate the temperature at which they are taken, *e.g.* $\kappa_t = \kappa(T_t)$ etc. $\Delta_t = T_c - T_t$ and $\Delta_b = T_b - T_c$ denote the temperature drops over the top and bottom thermal boundary layers, and λ_t^{sl} and λ_b^{sl} indicate their thicknesses, based on the temperature slopes at the top and bottom plates, respectively. λ_{OB}^{sl} is the thermal BL thickness in the OB case, both at top and at bottom. The factor F_Δ can be calculated from the temperature dependences of the material properties immediately, once T_c is known.

Remarkably, Ahlers *et al.* [6] experimentally found that for water

$$F_\lambda \approx 1. \tag{2}$$

This has been confirmed by numerical simulations of 2D NOB Rayleigh-Bénard convection in ref. [7]. If the relation eq. (2) holds, the Nusselt number ratio $\frac{Nu_{NOB}}{Nu_{OB}}$ already follows from the center temperature T_c, which for water can be calculated within a generalized boundary layer theory introduced in ref. [6].

The objective of this letter is to answer the apparently important question whether the relation $F_\lambda \approx 1$, meaning that the sum of the boundary layer thicknesses stays the same as in the OB case also under NOB conditions, $\lambda_b^{sl} + \lambda_t^{sl} \approx 2\lambda_{OB}^{sl}$, is more generally valid, *i.e.*, if it holds for other liquids too. We therefore have performed (two-dimensional) NOB simulations with glycerol as the working fluid. For glycerol the kinematic viscosity dramatically depends on temperature, *i.e.*, one should expect large changes of the boundary layer thicknesses at top and bottom. For instance, ν decreases from $1759\,\mathrm{mm}^2/\mathrm{s}$ to $52.5\,\mathrm{mm}^2/\mathrm{s}$ if the temperature increases from $15\,^\circ\mathrm{C}$ to $65\,^\circ\mathrm{C}$. Another advantage of considering glycerol is the existence of experimental data for the center temperature (see ref. [4]) for comparison (but not for the Nusselt number modification). Our main result will be that the sum of the boundary layer widths is indeed changed under NOB conditions, *i.e.*, relation (2) does *not* hold for glycerol. Its validity for water thus turns out to be coincidental, due to the specific temperature dependences of its material parameters for the chosen temperatures in the experiments of ref. [6].

Note that the fluid flow in glycerol is very different from that in water at the same Ra. Due to glycerol's huge Prandtl number of about $Pr \approx 2500$, the transition range between the onset of convection at Ra_c and the loss of spatial coherence in the flow is much more extended than for water or air, whose Prandtl numbers are of order one. While in air and in water this transitions range extends to about $Ra \approx 5 \cdot 10^7$ to 10^8, only beyond which there is turbulent convection in the bulk, this range extends to much larger Ra in glycerol, namely to Rayleigh numbers of order $Ra \approx 10^{12}$. Since the numerical calculations cover the range up to $Ra \approx 10^8$ only, all results refer to a fluid flow still having coherent structures.

To quantify these statements we use an averaged Kolmogorov length η_K as a measure for the scale of coherent structures in the flow, more precisely

$$\ell_{coh} = 10\ \eta_K = 10\ (\nu^3/\varepsilon_u)^{1/4}. \tag{3}$$

Here ε_u is the volume average of the energy dissipation rate of the flow for which the well-known exact relation $\varepsilon_u = \nu^3 L^{-4} Pr^{-2} Ra(Nu-1)$ holds. With this we obtain

$$\ell_{coh}/L = 10\ Pr^{1/2}\,(Ra(Nu-1))^{-1/4} \tag{4}$$

as an estimate for a volume-averaged relative coherence length. Taking $Nu(Ra, Pr)$ from the unified theory of refs. [8], one thus obtains an estimate of the coherence length as a function of Ra and Pr from eq. (4), see fig. 1. The main features of the coherence length are i) its pronounced explicit dependence on Pr (the implicit dependence via Nu is only weak). It is by about a factor $\sqrt{2500} = 50$ larger for glycerol than for gases or water. ii) Its Ra-dependence is approximately $\ell_{coh} \propto Ra^{-0.3}$.

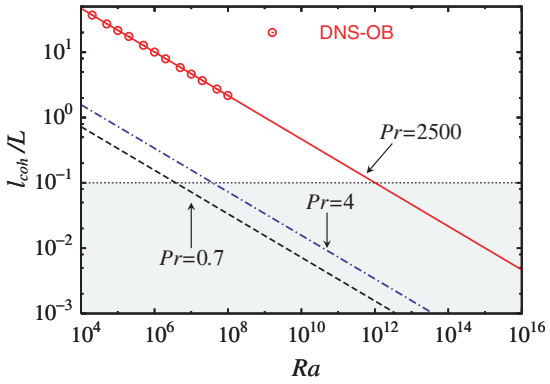

Fig. 1: (Color online) The coherence length ℓ_{coh} in multiples of the cell size L *vs.* Ra number for three fluids. For air and water it is of order 0.1 near $Ra \approx 10^7$ to $Ra \approx 10^8$. For glycerol this is reached much later; turbulent heat convection is expected beyond $Ra \approx 10^{12}$ only. Gray shaded region indicates the developed turbulent regime. Lines are derived from the unified theory of ref. [8], symbols correspond to the Rayleigh numbers of the present OB numerical simulations.

General description of numerical simulation. – We numerically solve the incompressible ($\partial_i u_i = 0$) Navier-Stokes equations

$$\rho_m(\partial_t u_i + u_j \partial_j u_i) = -\partial_i p + \partial_j(\eta(\partial_j u_i + \partial_i u_j)) + g\,(\rho_m - \rho)\,\delta_{i3}, \tag{5}$$

and the heat-transfer equation

$$\rho_m c_{p,m}(\partial_t T + u_j \partial_j T) = \partial_j(\Lambda \partial_j T). \tag{6}$$

The temperature dependence of the dynamic viscosity $\eta(T)$, the heat conductivity $\Lambda(T)$, and the density ρ are experimentally known for glycerol. They are given in the appendix of ref. [6]. As justified in that reference, we can assume the isobaric specific heat capacity c_p and the density ρ in the time derivatives of the material parameters to be constant at their values ρ_m and $c_{p,m}$ at the arithmetic mean temperature T_m. We vary the Rayleigh number Ra up to 10^8 and the level of the NOBness Δ up to $50\,\mathrm{K}$.

The container is two-dimensional (2D, no y-dependence), has height L, and aspect ratio 1. The flow is wall-bounded, *i.e.*, we use no-slip boundary conditions at all solid boundaries: $u_i = 0$ at the top ($z = L$) and bottom ($z = 0$) plates as well as on the side walls $x = 0$ and $x = L$. For the temperature at the side walls heat-insulating conditions are employed and $T_b - T_t = \Delta$

is the temperature drop across the whole cell. The Rayleigh number is defined with the material parameters taken at the mean temperature T_m, *i.e.*,$Ra = \frac{\beta_m g L^3 \Delta}{\nu_m \kappa_m}$. The arithmetic mean temperature is fixed at $T_m = 40\,^\circ$C. We vary the Rayleigh number by varying the height L of the box, while the NOBness is changed by varying the temperature drop Δ. Note that in the buoyancy term in eq. (5) the full temperature dependence of the density is taken into account, rather than employing the linear approximation $\rho(T) - \rho_m = \rho_m \beta (T - T_m)$ only. (Nevertheless, the Rayleigh number is defined as usual with the linear expansion coefficient of the density with respect to temperature, taken at T_m, namely $\beta_m = -\frac{1}{\rho_m}\frac{\mathrm{d}\rho}{\mathrm{d}T}|_{T_m}$.) The Prandtl number is defined as $Pr = \nu_m/\kappa_m$; for glycerol at the chosen temperature T_m its value is $Pr = 2495$. The basic equations are directly solved on the two-dimensional domain by means of the fourth-order finite difference method. For a detailed description of the simulation method as well as its validations, see ref. [7].

One may worry if two-dimensional simulations are sufficient to reflect the dynamics of the three-dimensional RB convection. For convection under OB conditions this point has been analyzed in detail in ref. [9] and earlier in refs. [10–13]. The conclusion is that for $Pr \gtrsim 1$ various properties observed in numerical 3D convection and in experiment are well reflected in 2D simulations. This in particular holds for the BL profiles and for the Nusselt number. Since the focus of this paper is on the difference between OB and NOB convection, the restriction to 2D simulations seems to be even less severe, as NOB deviations are expected to be similar in both 2D and 3D simulations and remaining differences to cancel out in quantities such as $T_c - T_m$ or Nu_{NOB}/Nu_{OB}.

Results and discussions. –

Large-scale flow dynamics and temperature snapshots. In the steady-flow regime ($Ra < 1.5 \cdot 10^5$) a single large-scale circulation role develops, which however disappears in the unsteady flow regime ($Ra > 1.5 \cdot 10^5$) and does not reappear up to the largest accessible value $Ra = 10^8$ of the present study. Even if we start the simulation with an artificial single roll, the large-scale circulation disappears in the course of time and then isolated plumes (as shown in fig. 2) dominate the flow. This feature holds for both cases, OB and NOB, and is qualitatively different from the observations in 2D (OB and NOB) simulations in water (see ref. [7]). We attribute this to the much larger spatial correlations in glycerol as addressed above. Note that in experiment (ref. [4]) for larger $Ra = 2.3 \cdot 10^8$ a large-scale 3D circulation role has been observed for glycerol. The different behavior between the present DNS and the experiment could either be due to the smaller Ra or to the two-dimensionality in the simulation.

Typical temperature snapshots are shown in fig. 2. As observed in experiments, refs. [4,6], the NOB convection is characterized by an enhancement of the bulk temperature

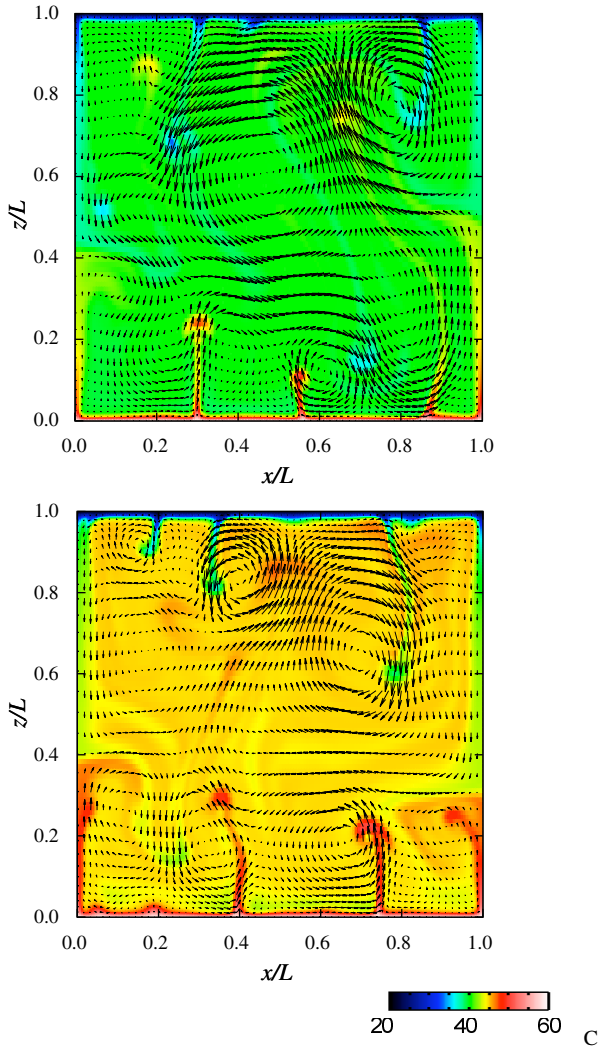

Fig. 2: (Color online) Snapshots of the velocity and temperature fields for $Ra = 10^8$ at $T_m = 40\,^\circ$C. The upper panel corresponds to the OB case (T-independent material parameters), the lower one to the NOB case, both with $\Delta = 40\,$K. The temperature color scheme is the same in both cases. In the NOB case a strong temperature enhancement of the center is clearly visible.

T_c, and a top-bottom asymmetry of the thermal BL thicknesses. Due to the large variation of the glycerol viscosity (the viscosity ratio reaches as much as $\nu_t/\nu_b \approx 16$ at $\Delta = 40\,$K), the more viscous cold plumes from the top BL are much less mobile than the warmer plumes from the bottom BL. This results in a significant increase of T_c as compared to the water case.

Mean-temperature profiles and center temperature. To quantify the enhancement of the bulk temperature T_c, the temperature profiles for $Ra = 10^8$ are shown in fig. 3. Again, a strong asymmetry between top and bottom is observed: Due to the more mobile bottom plumes the center temperature T_c is significantly larger than T_m.

To demonstrate this the center temperature shift $T_c - T_m$ (normalized by Δ) as function of the Rayleigh

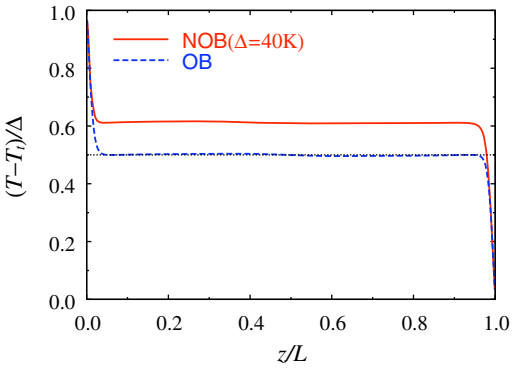

Fig. 3: (Color online) Mean temperature profiles for glycerol at $Ra = 10^8$ in the OB case (dashed) and in the NOB case with $\Delta = 40\,\mathrm{K}$ (solid). (In both cases $T_m = 40\,^\circ\mathrm{C}$, same Ra, same Δ, but T-independent (OB) or T-dependent (NOB) material parameters, respectively.) In the NOB case the strong temperature enhancement of the center temperature T_c by about 5 K becomes visible (relative shift ≈ 0.12).

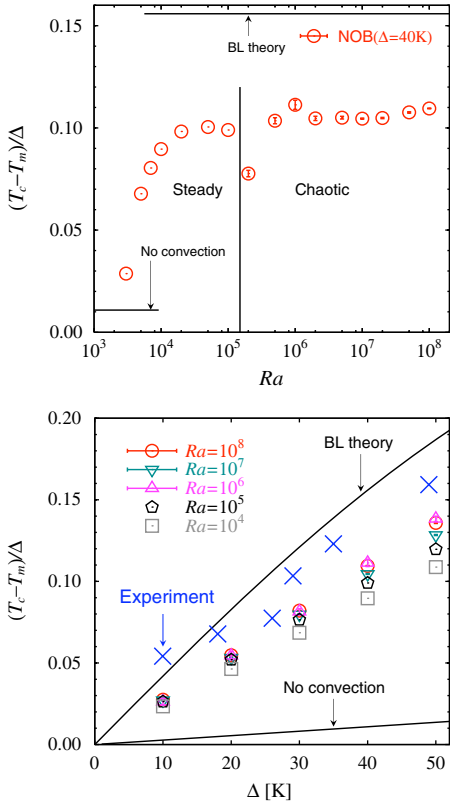

Fig. 4: (Color online) Relative deviation $(T_c - T_m)/\Delta$ of the center temperature T_c from the arithmetic mean temperature T_m for glycerol *vs.* Ra at fixed $\Delta = 40\,\mathrm{K}$ (upper panel) and *vs.* the NOBness Δ at fixed $T_m = 40\,^\circ\mathrm{C}$ and various values of Ra (lower panel). The experimental data points (denoted by $\times$) are measured at $Ra = 2.3 \cdot 10^8$ and were taken from ref. [4]. For comparison the T_c shift obtained from BL theory (upper solid lines) and for the case of no convection (lower solid lines) are also plotted.

number Ra and of the NOBness Δ is shown in fig. 4. Except for small Rayleigh numbers just above onset of convection and in a region around $Ra \approx 2 \cdot 10^5$ just above the onset of unsteady motion, the bulk temperature shift $(T_c - T_m)/\Delta$ is rather independent of Ra. The tiny increase between $Ra = 10^7$ and 10^8 however is beyond the statistical error-bars. For comparison, the prediction of the NOB BL theory given in ref. [6] and the shift for the non-convective state (*i.e.*, purely conductive heat transport, driven by the temperature gradient only) are shown. Though the NOB BL theory from ref. [6] is not applicable here due to the lack of a large-scale wind, it gives the correct qualitative trend for the shift $(T_c - T_m)/\Delta$. We also included experimental data measured at $Ra = 2.3 \cdot 10^8$ (taken from ref. [4]) in an aspect-ratio-1 cylindrical container. Though for that case a large-scale convection role has been observed, the agreement with the 2D numerical simulations is reasonable.

Nusselt number. The key question on NOB effects is: How do they affect the heat flux, *i.e.*, the Nusselt number? For water we could address this question within an extended BL theory, cf. ref. [6], but only thanks to the exact relation eq. (1) and the *experimental* input $F_\lambda \approx 1$, see relation (2), because then only F_Δ is needed to calculate the NOB deviations in the Nusselt number ratio, and F_Δ is accessible within the extended BL theory, since it follows directly from T_c. But here, with glycerol as working fluid, we find that $F_\lambda \approx 1$ does *not* hold, as demonstrated in fig. 5. In contrast to water, for glycerol the main Δ-dependence of $Nu_{NOB}/Nu_{OB} = F_\lambda \cdot F_\Delta$ is due to the Δ-dependence of F_λ while the factor F_Δ is basically 1 for all Δ's. This qualitative difference between glycerol and water in the origin of the Nusselt number modification also means that the experimental finding $F_\lambda \approx 1$ for water at $T_m = 40\,\mathrm{K}$ and Ra in the range of 10^8–10^{10}, see ref. [6], is merely accidental and not a general feature of the RB flow under NOB conditions.

Both NOB responses, the shift of the center temperature T_c and thus $\Delta_b \neq \Delta_t$ as well as the shift of the BL thicknesses $\lambda_{b,t}^{sl}$, are determined by the full nonlinear dynamics, in glycerol as well as in water. The T_c-shift in glycerol is even larger ($\approx 6.5\,\mathrm{K}$) than in water ($\approx 1\,\mathrm{K}$). The same is expected for the $\lambda_{b,t}^{sl}$-shifts. But the differences in the temperature drops $\Delta_{b,t}$ enter via F_Δ; here they are weighed with the explicit temperature dependence of the material parameter $\kappa(T)$. Since the thermal diffusivity changes only minutely in glycerol, $\kappa_{b,t}/\kappa_m - 1 \approx \pm 0.01$, the factor F_Δ stays near $F_\Delta \approx 1$ despite the large T_c response, cf. figs. 5, 6. This does not happen in F_λ; here the full changes of $\lambda_{b,t}^{sl}$ enter. Because of the very strong and in particular nonlinear temperature dependence of ν the thicknesses of the BLs change significantly and also quite differently in magnitude at the bottom and the top BLs, because $\sqrt{\nu_t/\nu_b} \approx 2.4$ due to the strong nonlinear T-dependence of $\nu(T)$. Therefore the sum $\lambda_b^{sl} + \lambda_t^{sl}$ no longer is equal to $2\lambda_{OB}^{sl}$. For water, instead, the

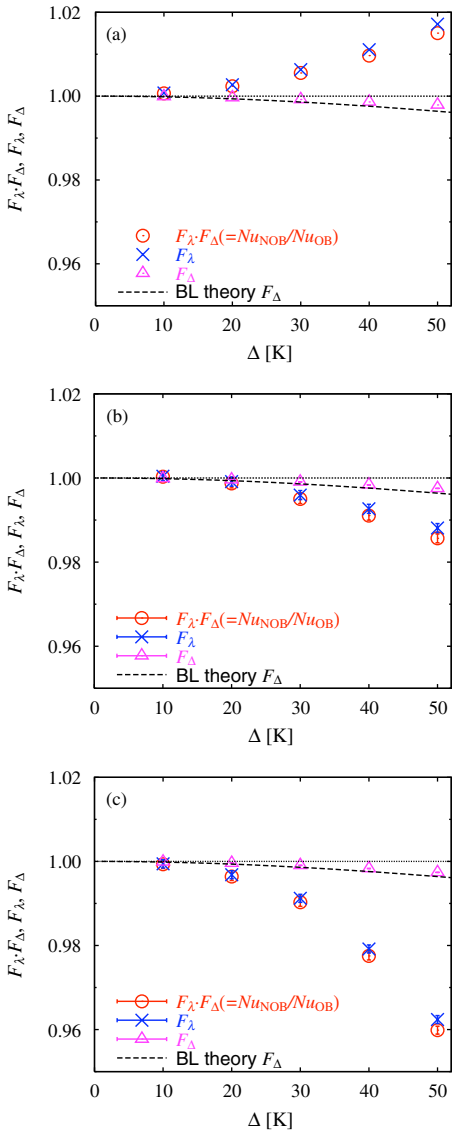

Fig. 5: (Color online) Nusselt number ratio $Nu_{NOB}/Nu_{OB} = F_\lambda \cdot F_\Delta$ together with its contributing factors F_λ and F_Δ *vs.* Δ for fixed Rayleigh numbers. (a) $Ra = 10^4$, (b) $Ra = 10^7$, and (c) $Ra = 10^8$. As always, the working liquid is glycerol at $T_m = 40\,^\circ$C. The dashed lines correspond to F_Δ resulting from the NOB BL theory of ref. [6].

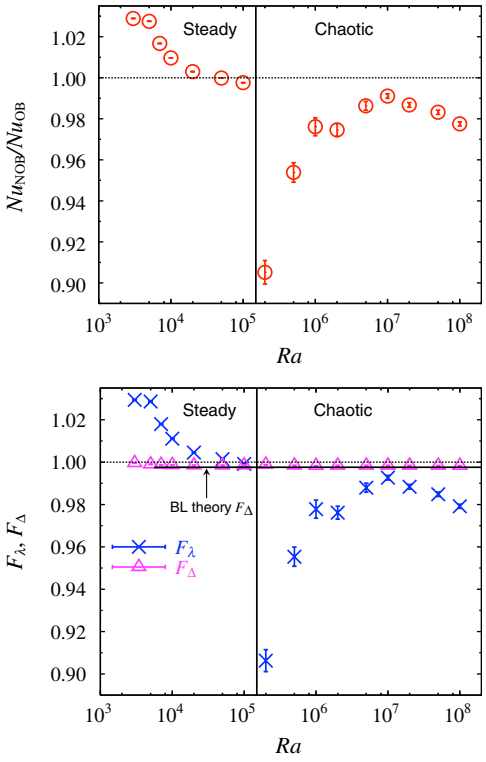

Fig. 6: (Color online) The Nusselt number ratio $Nu_{NOB}/Nu_{OB} = F_\lambda \cdot F_\Delta$ (upper panel) and the constituting factors F_λ and F_Δ individually (lower panel) *vs.* Ra for fixed NOBness $\Delta = 40\,$K (glycerol at $T_m = 40\,^\circ$C). Note the dramatic NOB effect at $Ra \approx 2 \cdot 10^5$; this happens still in the pattern forming range, far below the turbulent high Ra region. We are not aware of its experimental verification.

dominantly linear $\lambda^{sl}_{b,t}$-NOB modifications are opposite in sign and nearly cancel in the sum of the NOB thicknesses, giving $\lambda^{sl}_b + \lambda^{sl}_t \approx 2\lambda^{sl}_{OB}$ or $F_\lambda \approx 1$. Thus in glycerol we have $F_\Delta \approx 1$ and the Nu changes are dominated by F_λ, while in water it is $F_\lambda \approx 1$ and the NOB effects in Nu are determined dominantly by F_Δ (which is given by the temperature shift alone).

Figure 6 shows that the dependences of Nu_{NOB}/Nu_{OB} and F_λ on the Rayleigh number Ra are non-monotonous. We consider this as due to the nontrivial evolution of various coherent flow patterns with increasing Ra. In particular, as shown in fig. 5, for $Ra = 10^4$ the function $F_\lambda(\Delta)$ shows a qualitatively opposite behavior to that for water, namely F_λ increases with increasing Δ and reaches as large a value as 1.017 at $\Delta = 50\,$K. A consequence of our finding is that in general $Nu_{NOB}/Nu_{OB} = F_\lambda \cdot F_\Delta$ *cannot* be calculated within the extended BL theory introduced in ref. [6], even if a large-scale wind has formed: Within BL theory only the factor F_Δ can be calculated but not the factor F_λ, for which in general one cannot assume $F_\lambda \approx 1$.

We finally present our results for the Nu number itself as a function of Ra, see fig. 7, both for the OB and the NOB case. The inset shows the local scaling exponents. When applying the unifying theory of refs. [8], it is 0.306 at $Ra = 10^8$ and $Pr = 2500$, consistent with our numerical findings. This local slope practically does not change in the NOB case.

Summary and conclusions. – In summary, for glycerol both the center temperature T_c and the Nusselt number Nu of the 2D numerical simulations are in good agreement with the available experimental data of ref. [4]. The experimental finding by Ahlers *et al.* [6] of a "thermal-BL-thickness sum rule" for water, $F_\lambda \approx 1$ or $\lambda^{sl}_b + \lambda^{sl}_t \approx 2\lambda^{sl}_{OB}$, is shown to be incidental and seems due to the specific temperature dependence of the material parameters of water at 40 °C. Apparently this cannot

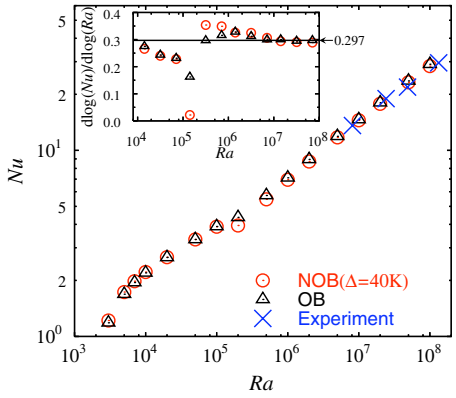

Fig. 7: (Color online) The Nusselt number Nu for glycerol *vs.* Ra under OB (dashed line) and NOB (solid line) conditions. In both cases $T_m = 40\,^\circ$C and $\Delta = 40$ K. OB is provided by keeping the material parameters artificially constant with T. We have also included the available data from ref. [4]. Logarithmic slope $\mathrm{d}\log(Nu)/\mathrm{d}\log(Ra)$ is plotted in the inset and the line corresponding to the exponent 0.297 measured in ref. [4] is also shown.

be generalized to other fluids (or other mean temperatures), as our analysis of RB convection in glycerol has shown. While for water the Nusselt number modification Nu_{NOB}/Nu_{OB} is due to the modified temperature drops over the BLs, represented by F_Δ, as shown in refs. [6,7], for glycerol it is governed by the variation of the BL thicknesses, namely by F_λ. This can be attributed to the strong and nonlinear temperature dependence of $\nu(T)$.

* * *

We thank G. Ahlers and F. Fontenele Araujo for many fruitfull discussions over the last years. The work in Twente is part of the research program of FOM, which is financially supported by NWO and SGn acknowledges support by FOM.

REFERENCES

[1] Oberbeck A., *Über die Wärmeleitung der Flüssigkeiten bei Berücksichtigung der Strömungen infolge von Temperaturdifferenzen, Ann. Phys. Chem.*, **7** (1879) 271.
[2] Boussinesq J., *Theorie analytique de la chaleur*, Vol. **2** (Gauthier-Villars, Paris) 1903.
[3] Wu X. Z. and Libchaber A., *Phys. Rev. A*, **43** (1991) 2833.
[4] Zhang J., Childress S. and Libchaber A., *Phys. Fluids*, **9** (1997) 1034.
[5] Ahlers G., Fontenele Araujo F., Funfschilling D., Grossmann S. and Lohse D., *Phys. Rev. Lett.*, **98** (2007) 054501.
[6] Ahlers G., Brown E., Fontenele Araujo F., Funfschilling D., Grossmann S. and Lohse D., *J. Fluid Mech.*, **569** (2006) 409.
[7] Sugiyama K., Calzavarini E., Fontenele-Araujo F., Grossmann S. and Lohse D., *Non-Oberbeck-Boussinesq effects on flow structure in Rayleigh-Bénard convection in water*, to be submitted to *J. Fluid Mech.* (2007).
[8] Grossmann S. and Lohse D., *J. Fluid. Mech.*, **407** (2000) 27; *Phys. Rev. Lett.*, **86** (2001) 3316; *Phys. Rev. E*, **66** (2002) 016305; *Phys. Fluids*, **16** (2004) 4462.
[9] Schmalzl J., Breuer M., Wessling S. and Hansen U., *Europhys. Lett.*, **67** (2004) 390.
[10] DeLuca E. E., Werne J., Rosner R. and Cattaneo F., *Phys. Rev. Lett.*, **64** (1990) 2370.
[11] Werne J., DeLuca E. E., Rosner R. and Cattaneo F., *Phys. Rev. Lett.*, **67** (1991) 3519.
[12] Werne J., *Phys. Rev. E*, **48** (1993) 1020.
[13] Burr U., Kinzelbach W. and Tsinober A., *Phys. Fluids*, **15** (2003) 2313.